

Multiple Andreev reflections in s-wave superconductor-quantum dot- topological superconductor tunnel junctions and Majorana bound states

Anatoly Golub

Department of Physics ,
Ben-Gurion University, Beer Sheva 84105 Israel

We calculate the current as a function of applied voltage in non-topological s-wave superconductor-quantum dot-topological superconductor tunnel junction (S-QD-TS). We consider the type of TS which hosts two Majorana bound states (MBS) at the ends of a semiconductor quantum wire or of a chain of magnetic atoms in the proximity with s-wave superconductor. We find that the I-V characteristic of such system in the regime of big voltages has a typical two dot shape and is ornamented by peaks of multiple Andreev reflections. We also consider the other options when the zero energy states are created by disorder (here by Shiba states) or by Andreev zero energy bound states at the surface of quantum dot and superconductor. The later are obtained by tuning the magnetic field to a specific value. Unlike the last two cases the MBS I-V curves are robust to change of magnetic field. Therefore, the magnetic field dependence of the tunneling current can serve as a unique signature for the presence of an MBS.

PACS numbers: 73.43.-f, 71.10.Pm, 74.45.+c, 73.23.-b

Introduction: In recent years the exotic Majorana bound state (MBS) is the focus of investigations in condensed matter physics. Different platforms for obtaining an MBS and variety of setups for experimental observation were suggested¹⁻⁹. In particular a zero bias peak in the conductance was predicted¹⁰⁻¹³. Recently¹⁴ Majorana fermions were observed at the edge of a topological superconductor (TS) which was formed by ferromagnetic chain placed in proximity to s-wave superconductor with strong spin-orbital interaction. The other of the leading candidates is semiconductor quantum wire in proximity to an s-wave superconductor - a system that generates a topological superconductor (TS) with two MBS's at its ends. A signature of a MBS in such a system has been detected in tunneling data in normal metal - TS junctions¹⁵⁻¹⁷, though the evidence is not conclusive¹⁸.

A setup has been suggested¹⁹ for detecting an Aharonov -Bohm (AB) interference between MBS and a quantum dot, predicting structure in the tunneling data. Furthermore, zero frequency shot noise has been studied²⁰⁻²². However, more evidence of a MBS is needed.

The modified subgap features as signatures of MBS due to multiple Andreev reflections in a weak link between two topological superconductors was addressed in²³. It has been shown theoretically that multiple Andreev reflection (MAR) in a weak link between two topological superconductors(i.e., hosting MBS) could cause novel subgap structures different from the trivial case which can also be regarded as signatures of MBS^{23,24}. The other more complicated setup was recently theoretically investigated in²⁵. There the electronic transport through a junction where a quantum dot (QD)is tunnel coupled on both sides to semiconductor nanowires with strong spin-orbit interaction and proximity-induced superconductivity is analyzed.

Here we consider a simpler case of a tunnel junction S-QD-TS where S stands for topologically trivial s-wave

superconductor and TS hosts one MBS at his tunneling end to the quantum dot. We study the case of large voltages V (though $eV < \Delta$) which permits to ignore constant phase-difference. We also assume that the charging energy of the dot is much smaller then Δ and therefore is ignored. We also consider weak tunneling limit when direct tunneling between superconductors is small and, therefore, multiple Andreev reflections due to these direct tunneling events are negligible in sub-gap region.

Including the QD change the situation: the transport current acquires a structure typical for two dot tunneling processes²⁶. However, we show that the contributions which come from MBS of TS can be easily distinguished from a random impurity zero energy states inside the gap of topologically trivial s-wave superconductor. As an example of a such impurity we take classical magnetic impurity with spin S (Shiba model^{27,28}). The Shiba resonance is strongly influenced by applied magnetic field. The same is true in other case of Andreev zero energy bound states which we also consider in details.

The Hamiltonian: The Hamiltonian of our system consists of topologically trivial s-wave superconductor lead part H_L , the quantum dot H_d and the tunnel couplings H_T Hamiltonian. The geometry is depicted in Fig. 1. Here t_R, t_L define the tunnel couplings between the MBS and dot, between the dot and the lead. $N(0)$ is the density of states of the lead in the normal state and the tunneling widths turn out to be $\Gamma_L = 2\pi N(0)t_L^2 \ll t_{L,R}$. The superconducting s-wave lead is placed at voltage bias V which is bigger compared to all other energy scales in the system, including Zeeman energy (though, V is less than the superconducting gap). We also assume that the MBS is well separated from other MBSs, e.g. at the other end of a TS wire, and therefore neglect the coupling between them. We write the Hamiltonian in spin (s matrices) and Nambu (particle- hole space, τ matrices)

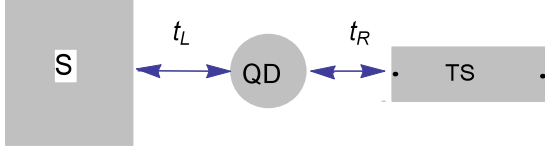


FIG. 1: Structure of the tunneling junction which consists of non-topological s-wave superconductor lead, embedded quantum dot and topological superconductor with Majorana fermion at its ends. The interaction couplings are presented. The phase $\phi = 2eVt$ (we have dropped constant phase).

as

$$\begin{aligned} H_d &= \frac{1}{2}d^\dagger(\varepsilon s_0 + H s_z) \times \tau_z d \\ H_T &= \frac{1}{2}[(t_L c^\dagger(0) + t_R \bar{V}^\dagger s_0) \times \tau_z d + h.c] \end{aligned} \quad (1)$$

where s_0, τ_0, s_i, τ_i ($i = x, y, z$) are unit and Pauli matrices, respectively, and $2H$ is the Larmor frequency, including the g factor. The Hamiltonian H_L of the superconducting lead has a standard form. The lead and dot electron operators are of the form $c = (c_\uparrow, c_\downarrow, c_\downarrow^\dagger, -c_\uparrow^\dagger)^T$ and the Majorana fermion operator γ comes with the spinor $\bar{V}_\varphi = (e^{i\varphi}, e^{i\varphi}, e^{-i\varphi}, -e^{-i\varphi})^T$, the φ is the constant phase. The average energy level of the dot is ε .

The current operator is defined as $J = e \frac{d}{dt} N_L = -ie[N_L, H]$ and acquires a form $J = (-i/4)j_d$ where

$$j_d = t_L[c^\dagger(0) \times \tau_0 d - h.c.] \quad (2)$$

We use the current in Keldysh a space^{29,30} (\hat{j}_d) to construct the effective action with source term. In the Keldysh theory the source field consists of two components: the classical α_{cl} and quantum one α . The classical part α_{cl} is irrelevant for noise and current calculations and we put it to zero. In this case the source action has a form

$$A_{sour} = \frac{1}{4} \int_t \alpha \hat{j}_d \quad (3)$$

Majorana bound states at ends of TS: At first we consider a case with TS as the right lead. The MBS states exist at the both ends of a topological superconductor. For sufficiently long TS only one MBS is involved in tunneling. After integrating out the lead and dot operators we arrive at the effective action in terms of Majorana Greens function (GF) which depends on coupling strengths and on quantum source field $\alpha(t)$

$$\begin{aligned} A_t &= \frac{1}{2} \int_t \gamma^T G_M^{-1} \gamma; \quad G_M^{-1} = G_{M0}^{-1} - \Sigma(\alpha) \\ \Sigma(\alpha) &= t_R^2 \bar{V}^\dagger \tau_3 G_d \tau_3 \bar{V} \end{aligned} \quad (4)$$

here $G_{M0}^{R,A}(E) = 1/(E \pm i\delta)$; the quantum dot GF $G_d(E) = [G_{d0}^{-1} - \Gamma_L g_T]^{-1}$ depends on left lead GF with included source term $g_T = T_- g T_+$, where

$$T_\pm = \tau_z \times \sigma_0 \pm \alpha \tau_0 \times \sigma_x / 2 \quad (5)$$

here $\sigma_{x,y,z}$ are the Pauli matrices in Keldysh space. In the limit $\alpha \rightarrow 0$ we obtain

$$G_d(E) = [G_{d0}^{-1} - \Gamma_L \tau_3 g \tau_3]^{-1} \quad (6)$$

The GF of noninteracting dot in magnetic field H has a form

$$G_{d0}^R(E) = [(E + i\delta)s_0 \times \tau_0 - \epsilon s_0 \times \tau_z - H s_z \times \tau_0]^{-1} \quad (7)$$

The Keldysh GFs of the lead

$$g = \begin{pmatrix} g^R & g^K \\ 0 & g^A \end{pmatrix} \quad (8)$$

in equilibrium ($V=0$) g^R has a form

$$g^R = \frac{-i}{2} [a(E)s_0 \times \tau_0 + b(E)s_0 \times \tau_1] \quad (9)$$

$$a(E) = \frac{|E|\theta(|E| - \Delta)}{\sqrt{E^2 - \Delta^2}} + \frac{E\theta(\Delta - |E|)}{i\sqrt{\Delta^2 - E^2}} \quad (10)$$

$$b(E) = \frac{\Delta}{E} a(E) \quad (11)$$

where $\theta(x)$ is step function equal to one if $x > 0$ and is zero otherwise. The energy gap Δ describes the lead presented by topologically trivial s-wave superconductor. Advanced function (A) is equal to the adjoint of given retarded function; and $g^K(E) = (g^R(E) - g^A(E)) \tanh(E/2T)$.

Off-diagonal GF of s-wave superconductor depends on phase of the order parameter $\exp[\pm i\phi(t)] = \exp[\pm i2eVt]$. Therefore, at nonzero voltage V we have a Floquet periodic time dependent problem with a basic frequency $\omega_0 = 2eV$. Superconducting lead (topologically trivial) under fixed voltage is described by time dependent GFs. Their Fourier-transforms are expressed in terms of equilibrium ones (a generalization to 4×4 dimension of the relations from reference³¹)

$$\begin{aligned} g(E, E) &= g_{11}(E - eV)s_0 P_+ + g_{22}(E + eV)s_0 P_- \\ g(E, E - 2eV) &= g_{21}(E - eV)s_0 \tau_+ \\ g(E, E + 2eV) &= g_{12}(E + eV)s_0 \tau_- \end{aligned} \quad (12)$$

where $P_\pm = (\tau_0 \pm \tau_3)/2$, $\tau_\pm = \frac{1}{2}(\tau_x \pm \tau_y)$. The lead GF g may by any function (R,A, or K). We have dropped a constant phase which is justified for not too small voltages. A complete representation of GFs in Floquet basis is presented in the supplementary material.

We evaluate the current by taking derivatives of the effective action with respect to α and use dimensionless notations: all energies are taken in units of Δ . The total dc current is given by three contributions

$$j/j_0 = \frac{t_R^2 \Gamma_L}{2\Delta^3} (j_1 + j_2 + j_3) \quad (13)$$

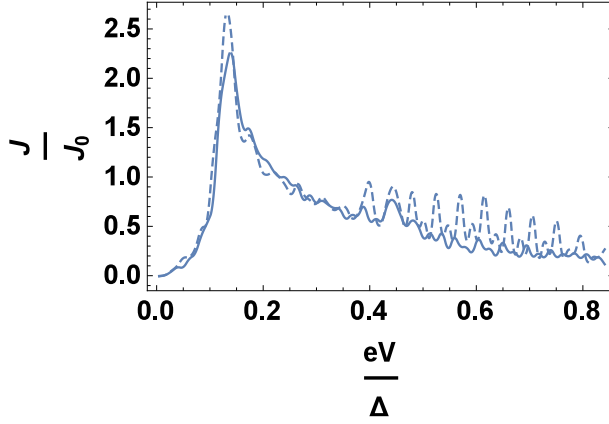


FIG. 2: Current -voltage characteristics of the tunnel junction (Fig.1). The dot energy $\epsilon = -0.01\Delta$, the temperature $T = 0.1\Delta$; the tunneling widths $\Gamma_L/\Delta = 0.02$ and $t_R^2/\Delta^2 = 0.2$. The lines correspond to zero magnetic field (solid) and $H = 0.1\Delta$ (dashed).

where $j_0 = e/(2\Delta)$ and j_1, j_2, j_3 are expressed in terms of Majorana, quantum dot and left lead GFs (see supplementary material).

We calculate the I-V characteristics of a setup (Fig1) in the sub-gap region and consider zero and nonzero magnetic field (Zeeman energy $H = 0.1\Delta$). It is known that in a low transparency SNS junctions the subgap current is small (approaching zero value)^{24,31}. The tunneling through the dot between superconducting leads is responsible for multiple Andreev reflections (MAR) which contributes to the current. The MBS states, acting as the other dot, however, being structureless (mixing the spin) are quite robust to the magnetic field. Thus we obtained (Fig.2) typical for two dots I-V curves²⁶. However, unlike the non-topological case have different peak position and in the whole subgap region I-V characteristics weakly depend on magnetic field. To obtain the I-V characteristics the number of Floquet states ($2n$) is adjusted until the result is insensitive to farther increase in n . The calculations include 12 Floquet states.

Impurity Zero mode in the gap (no-MBS): To prove that we have clear difference between topological and non-topological cases in this section we study the current for trivial topology but when, nevertheless, the zero bound states exists. This may be caused either by Andreev bound states or localized by disorder states (impurity), or by surface state as in a d-wave superconductor³². We investigate the I-V characteristics in the case of single Shiba resonance^{27,28} when it is tuned to form in-gap zero energy bound states^{33,34}. For a single impurity in the host superconductor lead (with $V=0$) the scattering problem can be easily solved^{27,28,33,34}. We consider a single (classical) magnetic impurity with spin S at the origin, interacting with the electron states

$$H_{imp} = -J\vec{S}c_R\vec{s} \times \tau_0 c_R(0)$$

where J is exchange strength and c_R stands for electron operator in the right superconductor. If we define the spin vector as $\vec{S} = (sin\theta cos\phi, sin\theta sin\phi, cos\theta)$, then at zero order in tunneling strength t_R , Green function G_{s0} of the right lead acquires a form (in dimensionless units, and for the frequencies less than the superconducting gap Δ i.e. $|E| < 1$)

$$(2G_{s0}^R(E))^{-1} = \frac{E}{\sqrt{1-E^2}}s_0 \times \tau_0 + \bar{\alpha} \cos\theta s_z \times \tau_0 - \frac{1}{\sqrt{1-E^2}}s_0 \times \tau_x - H s_z \times \tau_0 + \bar{\alpha} \cos\phi \sin\theta s_x \times \tau_0 + \bar{\alpha} \sin\phi \sin\theta s_y \times \tau_0 \quad (14)$$

where $\bar{\alpha} = \pi N_R J S$ is the dimensionless impurity interaction and N_R is the density of electron states in the right lead. We did not take in consideration Rashba spin orbit interaction, though, the result for single impurity is similar to the case without spin-orbit scattering³⁴. It was shown³³ and this can be directly checked by setting to zero the determinant of the matrix (14) that at $\bar{\alpha} \rightarrow 1$ and $H \rightarrow 0$ we arrive at the zero energy bound states. In the low energy domain close to the in-gap zero mode we can consider G_{s0} at small E . For voltages less than Δ this level defines transport. The tunneling interaction with the dot is described by the same Hamiltonian H_T (1) where instead of γV^+ we write projected to low energy domain electron operator f^\dagger . As in the case of MBS we integrate out the electron operators of both left lead and quantum dot. Thus we arrive at a general form of the effective action and GF which include interaction with the quantum dot.

$$G_s^{-1} = G_{s0}^{-1} - t_R^2 G_d \quad (15)$$

The current consists of a three contributions similar to those in Eqs.(A7) (see Supplement) however, there is an important difference: The Majorana GF is replaced by GF of Shiba resonance G_s . In equilibrium $G_{s0}^R(E)$ (14) is a 4×4 matrix in spin and Nambu spaces. In Floquet basis this matrix has a dimension $4(1+2n) \times 4(1+2n)$ and trace (see supplementary material) operates in this dimension. We calculate the current taking in consideration 12 Floquet states ($n=6$) using the same set of parameters as in the case of MBS. In Fig.3 we see shift of a much stronger peak of transport current as the magnetic field is switched on. This does not occur in MBS case. Therefore, the peak position and a stronger dependence of its value on magnetic field can serve as possible method to distinguish the Shiba resonance from MBS.

Andreev Zero Bound States (AZBS): Andreev bound states can appear in a system like ours when quantum dot contacts with superconductor. The zero energy limit mimics the MBS and may be obtained by proper tuning the Zeeman energy. Let us consider a setup like presented by Fig.1 where, however, instead of topological superconductor on the right hand side we have s-wave superconductor which is grounded. By tuning the magnetic

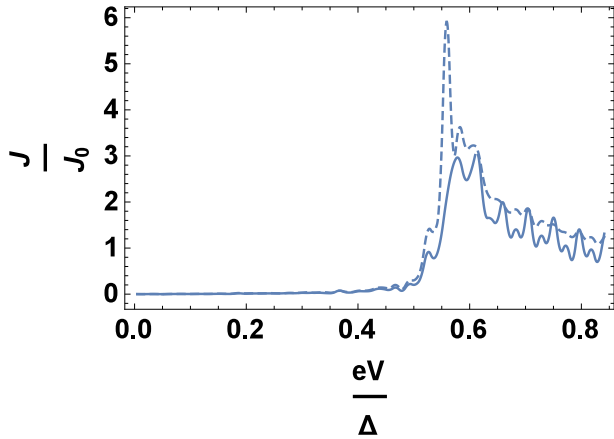


FIG. 3: The same as in Fig2. where , however, the TS is replaced by Shiba resonance at $\bar{\alpha} \rightarrow 1$. For this figure we took direction angles : $\phi = 0, \theta = \pi/2$. The other parameters are as in Fig.2.

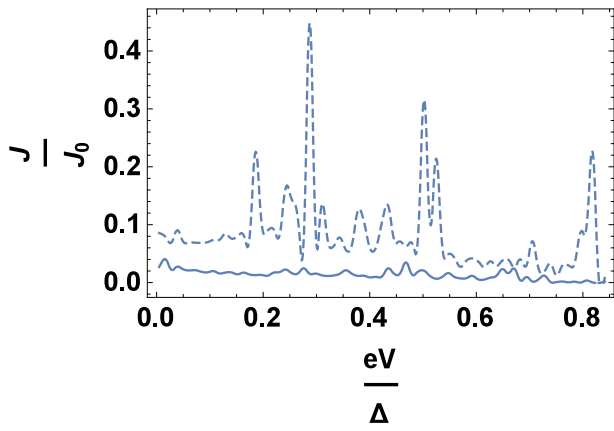


FIG. 4: The tunneling current versus voltage in the case of formation of AZBS at $H = H_0$ (dashed curve) and at $H=0$ when AZBS are depressed (solid line). The other parameters: the dot energy $\epsilon = -0.4\Delta$, the temperature $T = 0.03\Delta$; the tunneling widths $\Gamma_L/\Delta = 0.2$ and $\Gamma_R/\Delta = 0.3$

field we intend to get the low energy subspace due to interaction with s-wave superconductor, i.e., we associate AZBS only with s-wave superconductor which couples to quantum dot. Integrating out the electron operators of superconductors (left lead and right) we obtain total GF G_t of the dot which includes interactions with both superconductors. Actually, G_t has a form of Eq.(6), though, G_{d0} is replaced by G_{t0}

$$G_{t0}^{-1R}(E) = (E + \frac{\Gamma_R E}{2\sqrt{\Delta_R^2 - E^2}} + i\delta) s_0 \times \tau_0 - \epsilon s_0 \times \tau_z - H s_z \times \tau_0 - \frac{\Gamma_R \Delta_R}{2\sqrt{\Delta_R^2 - E^2}} s_0 \tau_x \quad (16)$$

were we, anticipating low energy domain, consider only the case $|E| < \Delta_R$. It is a direct way to show (by finding the roots of equation $\det[G_{t0}^{-1R}] = 0$) that the zero energy bound state can appear when we tune Zeeman energy to the value $H = H_0 = \sqrt{\Gamma_L^2/4 + \epsilon^2}$.

We compute the transport current (Eg.16 of supplementary material) and find the I-V characteristics of the junction (Fig.4). We can clearly distinguish AZBS which are created at magnetic field $H = H_0$ from the case when such a states are absent $H \neq H_0$ (here $H=0$). Many resonances which are shown on Fig.4 correspond to shifted by Floquet number the zero energy pole of GF (16). Moreover, AZBS, though, can mimic the resonance due to MBS, this resemblance may be destroyed by magnetic field different from H_0 .

Conclusion: We have applied the standard Keldysh technique^{29,30} to evaluate the tunneling current in a setup presented by Fig.1. As a specific example we consider a Majorana fermion at the end of a quantum wire which is placed in proximity with a superconductor and under an applied external magnetic field^{5,6}. Evidently, control of the magnetic field and the dot-MBS coupling t_R can provide a sensitive test for the MBS detection and may help to distinguish MBS from others zero bound states¹⁸ caused either by Andreev bound states or localized by disorder states, or by surface states as in d wave superconductors³². The difficulty with experimental identification of a MBS via the method of a zero bias conduction peak^{15–18} is that similar peaks may be due to other low energy bound states³⁷ such as states localized by disorder³⁵. However, on the experiment¹⁴ a chain of interacting magnetic iron atoms (magnetic dots) on superconducting lead was investigated. For this system which includes Hubbard interaction in the dot³⁶ the theory³⁵ is not directly applied.

We provide the solution of three models: one with MBS, the other one is a model in which the MBS is replaced by Shiba impurity resonance, and the last model represents the AZBS that can appear at the contact of quantum dot and s-wave superconductor at the specific value of Zeeman energy. We consider multiple Andreev reflections which are beyond the small voltage regime. We show that for last two (not with MBS) models zero localized states may be identified by strong peak dependence on magnetic field. A further difficulty with experimental identification is due to the accuracy with which a zero energy state can be determined, as function e.g. of a magnetic field^{16,17,37,38}. Therefore, control of the magnetic field and the dot-MBS coupling t_R provide an option for an MBS detection

I would like to thank B. Horovitz for stimulating discussions. This research was supported by the ISRAEL SCIENCE FOUNDATION (BIKURA) (grant No. 1302/11).

¹ A. Y. Kitaev, Physics-Uspekhi **44**, 131 (2001).
² L. Fu and C. L. Kane, Phys. Rev. Lett. **100**, 096407 (2008).
³ L. Fu and C. L. Kane, Phys. Rev. B**79**, 161408 (2009).
⁴ J.D. Sau, R. M. Lutchyn, S. Tewari, and S. Das Sarma, Phys. Rev. Lett. **104**, 040502 (2010).
⁵ R. M. Lutchyn, J. D. Sau, and S. Das Sarma, Phys. Rev. Lett. **105**, 077001 (2010).
⁶ Y. Oreg, G. Refael, and F. von Oppen, Phys. Rev. Lett. **105**, 177002 (2010).
⁷ J. Alicea, Phys. Rev. B**81**, 125318 (2010).
⁸ J. Linder, Y. Tanaka, T. Yokoyama, A. Sudbo, and N. Nagaosa, Phys. Rev. Lett. **104**, 067001 (2010).
⁹ J. Alicea, Rep. Prog. Phys. **75**, 076501 (2012).
¹⁰ A. R. Akhmerov, J. Nilsson, and C. W. J. Beenakker, Phys. Rev. Lett. **102**, 216404, (2009).
¹¹ K. T. Law, P. A. Lee, and T. K. Ng, Phys. Rev. Lett. **103**, 237001 (2009).
¹² Y. Tanaka, T. Yokoyama, and N. Nagaosa, Phys. Rev. Lett. **103**, 107002 (2009).
¹³ K. Flensberg, Phys. Rev. B**82**, 180516(R) (2010).
¹⁴ S. Nadj-Perge, I. K. Drozdov, J. Li, H. Chen, S. Jeon, J. Seo, A. H. MacDonald, B. A. Bernevig and A. Yazdani Science **346**, 6209 (2014). 107002 (2009).
¹⁵ V. Mourik, K. Zuo, S. M. Frolov, S. R. Plissard, E. P. A. M. Bakkers, and L. P. Kouwenhoven: Science **336** 1003 (2012).
¹⁶ A. Das, Y. Ronen, Y. Most, Y. Oreg, M. Heiblum and H. Shtrikman, Nature Phys. **8**, 887 (2012).
¹⁷ S. Sasaki, M. Kriener, K. Segawa, K. Yada, Y. Tanaka, M. Sato, and Y. Ando: Phys. Rev. Lett. **107** 217001 (2011).
¹⁸ E. J. Lee, X. Jiang, M. Houzot, R. Aguado, C. M. Lieber and S. De Franceschi, Nature Nanotechnology **9**, 79 (2014).
¹⁹ A. Ueda, T. Yokoyama, Phys. Rev. B**90**, 081405(R) (2014); arXiv:1403.4146.
²⁰ C. J. Bolech, Eugene Demler, Phys. Rev. Lett. **98**, 237002 (2007).
²¹ A. Golub and B. Horovitz, Phys. Rev. B**83**, 153415 (2011); and arXiv:1407.5179
²² K. Ya. M. Blanter and M. Büttiker, Physics Reports **336**, 1 (2000).
²³ D.M. Badiane, M. Houzet, and J.S. Meyer, Phys. Rev. Lett. **107**, 177002 (2011); http://arxiv.org/abs/1108.3870.
²⁴ P. San-Jose, J. Cayao, E. Prada and R. Aguado, New J. Phys. **15**, 075019 (2013).
²⁵ Guang-Yao Huang, M. Leijnse, K. Flensber, and H. Q. Xu, arXiv:1411.1225.
²⁶ L. P. Kouwenhoven, C. M. Marcus, P. L. McEuen, S. Tarucha, R. M. Westervelt, and N. S. Wingreen , "Mesoscopic Electron Transport" NATO ASI Series Volume 345, 1997, pp 105-214.
²⁷ H. Shiba, Prog. Theor. Phys. **40**, 435 (1968).
²⁸ A. I. Rusinov, Zh. Eksp. Teor. Fiz. Pisma Red. **9**, 146 (1968) [JETP Lett. **9**, 85 (1969)].
²⁹ L. V. Keldysh, Zh. Eksp. Teor. Fiz., **47**, 1515 (1965).
³⁰ A. Kamenev, A. Levchenko, Advances in Physics **58**, 197 (2009), arXiv:0706.3016 (2007).
³¹ G. B. Arnold Journal Low Temp. Phys. **59** 143 (1985).
³² B. Horovitz and A. Golub, Phys. Rev. B**68**, 214503 (2003)
³³ F. Pientka, L. I. Glazman, and F. von Oppen, Phys. Rev. B **88**, 155420 (2013).
³⁴ P. M. R. Brydon, Hoi-Yin Hui, and Jay D. Sau arXiv:1407.6345.
³⁵ D. Bagrets and A. Altland, Phys. Rev. Lett. **109**, 227005 (2012); A. Altland and M. R. Zirnbauer Phys. Rev. B**55**, 1142 (1997).
³⁶ J. Klassen, and Xiao-Gang Wen, arXiv:1412.5985 227005 (2012).
³⁷ J. Liu, A. C. Potter, K.T. Law, and P.A. Lee, Phys. Rev. Lett., **109**, 267002 (2012)
³⁸ S. De Franceschi, L. Kouwenhoven, C. Schnenberger, and W. Wernsdorfer Nature Nanotechnology, **5**, 703 (2010)

Appendix A: Supplemental Material

1. Greens functions in Floquet space

Here we obtain the matrices in Floquet space for nonequilibrium GFs of the left lead (superconductor), Majorana and dot Green functions (Eq.4 and Eq.6). Let us consider $2N + 1$ Floquet states. Definitions of GFs (Eq.12) show that the energy difference between the initial and final states is the integer multiple of $2eV$. To simplify notations we define $I = \text{integer}[\frac{i-1}{4}]$; $K = \text{integer}[\frac{k-1}{4}]$ and $E_K = E - 2eV(N - K)$, where $i, k = 1, 2, \dots, 4(2N + 1)$. Thus we have

$$\begin{aligned}
 g_{i,k}(E) &= g_d[i, k] + g_+[i, k] + g_-[i, k] \\
 g_d[i, k] &= \delta_{I,K} \{g_{11}(E_K - eV)s_0P_+ + g_{22}(E_K + eV)s_0P_-\}_{i-4K, k-4K} \\
 g_+[i, k] &= \delta_{I,K-1} g_{21}(E_K - eV) \{s_0\tau_+\}_{i-4(K-1), k-4K} \\
 g_-[i, k] &= \delta_{I,K+1} g_{12}(E_K + eV) \{s_0\tau_-\}_{i-4(K+1), k-4K}
 \end{aligned} \tag{A1}$$

The matrix structure of $4(2N + 1) \times 4(2N + 1)$ matrix $g_{i,k}(E)$ consists of 4×4 diagonal boxes (g_d) and of 4×4 blocks g_{\pm} on each side of diagonal. The other Keldysh GFs have similar representation. The dot GF (Eq.6) includes the lead GF g as its non-equilibrium part, therefore, we can write total inverse dot GF in the form like g (Eq.A1)

$$\begin{aligned}
 G_{di,k}^{-1R}(E) &= G_1[i, k] + G_+[i, k] + G_-[i, k] \\
 G_1[i, k] &= \delta_{I,K} \{E_K s_0 \tau_0 - \epsilon s_0 \tau_z - H s_z \tau_0 - \Gamma_L [g_{11}(E_K - eV)s_0P_+ + g_{22}(E_K + eV)s_0P_-]\}_{i-4K, k-4K}
 \end{aligned} \tag{A2}$$

$$\begin{aligned} G_+[i, k] &= \delta_{I, K-1} \Gamma_L g_{21}(E_K - eV) \{s_0 \tau_+\}_{i-4(K-1), k-4K} \\ G_-[i, k] &= \delta_{I, K+1} \Gamma_L g_{12}(E_K + eV) \{s_0 \tau_-\}_{i-4(K+1), k-4K} \end{aligned}$$

The dot GF $G_{di,k}$ is obtained by taking inverse of Eq.(A2).

Total Majorana GF, though, depends on dot function G_d (Eq.A4) has no spin and particle-hole presentation. It is a matrix only in Floquet space $(2N+1) \times (2N+1)$. Using definition of spinor $\hat{V}_{\varphi=0}$ (see Eq.1 and Eq.4) we find

$$G_{Mp,q}^{-1R}(E) = G_{M0p,q}^{-1R}(E) - \Sigma_{p,q}^R(E) \quad (\text{A3})$$

$$G_{M0p,q}^{-1R}(E) = \delta_{p,q} \{E - 2eV(N-p)\}$$

$$\begin{aligned} \Sigma_{p,q}^R(E) &= t_R^2 \{G_{d1+4p,1+4q}^R(E) + G_{d2+4p,2+4q}^R(E) + G_{d3+4p,3+4q}^R(E) + G_{d4+4p,4+4q}^R(E) + \\ &G_{d1+4p,3+4q}^R(E) - G_{d2+4p,4+4q}^R(E) + G_{d3+4p,1+4q}^R(E) - G_{d4+4p,2+4q}^R(E) - \\ &G_{d1+4p,4+4q}^R(E) + G_{d2+4p,3+4q}^R(E) + G_{d3+4p,2+4q}^R(E) - G_{d4+4p,1+4q}^R(E) + \\ &G_{d1+4p,2+4q}^R(E) + G_{d2+4p,1+4q}^R(E) - G_{d3+4p,4+4q}^R(E) - G_{d4+4p,3+4q}^R(E)\} \end{aligned} \quad (\text{A4})$$

here $p, q = 0, 1, 2, \dots, 2N$. Inverting Eq.(A3) we arrive at the effective Majorana GF.

The inverse GF of Shiba states in the low energy limit close to the in-gap zero (at $\tilde{\alpha} = 1$) replaces Majorana GF $G_{M0p,q}(E)$ in the expressions for tunneling current. Effective Shiba states Green's function (Eq.15) has the self-energy part which is determined by interaction with the dot. In Floquet basis this GF is $4(2N+1) \times 4(2N+1)$ matrix which has a form

$$G_{sp,q}^{-1R}(E) = G_{s0i,k}^{-1R}(E) - t_R^2 G_{di,k}^R(E) \quad (\text{A5})$$

$$G_{s0i,k}^{-1R}(E) = \delta_{I,K} \{E_K s_0 \tau_0 - \epsilon s_0 \tau_z - H s_z \tau_z + \cos \theta s_z \tau_0 + \cos \phi \sin \theta s_x \tau_0 + \sin \phi \sin \theta s_y \tau_0\}_{i-4K, k-4K} \quad (\text{A6})$$

2. The tunneling current

Let us at first to consider the tunneling current in S-QD-TS(MBS) junction. We evaluate the current by taking derivatives of the effective action with respect to α

$$j(t) = \frac{e}{4} \text{Tr} \int dt_1 \int dt_2 G_M(t_1 t_2) \left(\frac{\delta \Sigma(\alpha t_2 t_1)}{\delta \alpha(t)} \right)_{\alpha \rightarrow 0} \quad (\text{A7})$$

where Tr acts in Keldysh space. Explicitly the derivative acquires a form

$$\frac{\delta \Sigma(\alpha t_2 t_1)}{\delta \alpha(t)} = t_R^2 \Gamma_L \int dt_3 \int dt_4 \hat{V}^\dagger G_d(t_2 t_3) \frac{\delta g_T(t_3 t_4)}{\delta \alpha(t)} G_d(t_4 t_1) \hat{V} \quad (\text{A8})$$

$$\left(\frac{\delta g_T(t_3 t_4)}{\delta \alpha(t)} \right)_{\alpha \rightarrow 0} = \frac{1}{2} [g(t_3, t) \delta(t - t_4) \sigma_x \tau_z - \sigma_x \tau_z \delta(t - t_3) g(t, t_4)] \quad (\text{A9})$$

Performing the trace in Keldysh space we obtain several contributions to the current where, in addition to retarded and advanced GFs, the Keldysh component of GF is also involved. From Eqs.4,6 we obtain for these GFs:

$$G_M^K = t_R^2 G_M^R \hat{V}^\dagger \tau_z G_d^K \tau_z \hat{V} G_M^A \quad (\text{A10})$$

$$G_d^K = \Gamma_L G_d^R \tau_z g^K \tau_z G_d^A \quad (\text{A11})$$

We consider the time averaged transport current. Only zero multiple of $2eV$ in the Fourier series contributes to the current. In this case we use Fourier transform representation of GFs (A2,A3). The current is presented by a trace of proper combinations of these functions in Floquet space. Inserting the expressions Eq.(A8) and (A9) into Eq.(A7), performing the trace in the Keldysh space we arrive at final form of current in S-QD-TS(MBS) junction. The total dc current is given by three contributions where for last two we use Green Functions Eq.(A10,A11)

$$j/j_0 = \frac{t_R^2 \Gamma_L}{2\Delta^3} (j_1 + j_2 + j_3) \quad (\text{A12})$$

where $j_0 = e/(2\Delta)$ and j_1, j_2, j_3 acquire a form

$$j_1 = \text{tr} \int dE \text{Re} [G_M^R \bar{V}^+ \tilde{G}_d^R g^K \tau_z \tilde{G}_d^R \bar{V}] \quad (\text{A13})$$

$$j_2 = \frac{\Gamma_L}{\Delta} \text{tr} \int dE \text{Re}[G_M^R \bar{V}^+ \tilde{G}_d^R g^K \tilde{G}_d^A (g^A \tau_3 - \tau_3 g^R) \tilde{G}_d^R \bar{V}] \quad (\text{A14})$$

$$j_3 = \frac{\Gamma_L t_R^2}{2\Delta^3} \text{tr} \int dE \text{Re}[G_M^R \bar{V}^+ \tilde{G}_d^R g^K \tilde{G}_d^A \bar{V} G_M^A \bar{V}^+ \tilde{G}_d^A (g^A \tau_3 - \tau_3 g^R) \tilde{G}_d^R \bar{V}] \quad (\text{A15})$$

Here $\tilde{G}_d^{R,A} = \tau_3 G_d^{R,A} \tau_3$; tr stands for the trace over Floquet states; $G_M^{R,A}$ are the matrices in Floquet basis of dimension $(1+2N) \times (1+2N)$, the same as the blocks $[\bar{V}^+ \dots \bar{V}]$.

This fact is principal: it distinguishes topological case (with TS and MBS) from trivial normal zero level states inside the gap (here AZBS and Shiba resonance). Indeed the expression for the current in the case of Shiba zero states (i.e. we consider a junction S-QD-S(with Shiba state) coincides with Eq.(A13,A14,A15) if: (i) we replace Majorana GFs G_M by GFs of Shiba zero states; (ii) drop spinors \bar{V}^+, \bar{V} ; and (iii) take trace over the space $4(2N+1) \times 4(2N+1)$.

We also calculate the current in the case of Andreev zero energy bound states (AZBS). The transport current through the dot in a setup like shown on Fig1 of main text is described by Eq.(7) where instead of G_M and Σ we have $G_t = [G_{t0} - \Sigma_g]^{-1}$ and Σ_g correspondingly, and

$$\frac{\delta \Sigma_g(t_2 t_1)}{\delta \alpha(t)} = \Gamma_L \left(\frac{\delta g_T(t_2 t_1)}{\delta \alpha(t)} \right)_{\alpha \rightarrow 0} \quad (\text{A16})$$

With the help of Eq.16 and Eq.A9 we obtain

$$j/j_0 = \frac{\Gamma_L}{\Delta} \text{tr} \int dE \text{Re}[G_t^R \tau_z g^K (1 + \Gamma_L \tilde{G}_t^A g^A)] \quad (\text{A17})$$

where $\tilde{G}_t^A = \tau_z G_t^A \tau_z$ and trace acts in the space $4(2N+1) \times 4(2N+1)$.